





COVID-19 Variant Detection with a High-Fidelity CRISPR-Cas12 Enzyme

Clare L. Fasching,^a Venice Servellita,^{b,c} Bridget McKay,^a Vaishnavi Nagesh,^a James P. Broughton,^a Alicia Sotomayor-Gonzalez,^{b,c} Baolin Wang,^{b,c} Noah Brazer,^{b,c} Kevin Reyes,^{b,c} Jessica Streithorst,^{b,c} Rachel N. Deraney,^a Emma Stanfield,^a Carley G. Hendriks,^a Becky Fung,^b  Steve Miller,^{b,c} Jesus Ching,^a Janice S. Chen,^a  Charles Y. Chiu^{b,c,d}

^aMammoth Biosciences, Inc., Brisbane, California, USA

^bDepartment of Laboratory Medicine, University of California San Francisco, San Francisco, California, USA

^cUCSF-Abbott Viral Diagnostics and Discovery Center, San Francisco, California, USA

^dDepartment of Medicine, Division of Infectious Diseases, University of California San Francisco, San Francisco, California, USA

Clare L. Fasching and Venice Servellita contributed equally to this article. The author order was determined by the corresponding author after negotiation.

ABSTRACT Laboratory tests for the accurate and rapid identification of SARS-CoV-2 variants can potentially guide the treatment of COVID-19 patients and inform infection control and public health surveillance efforts. Here, we present the development and validation of a rapid COVID-19 variant DETECTR assay incorporating loop-mediated isothermal amplification (LAMP) followed by CRISPR-Cas12 based identification of single nucleotide polymorphism (SNP) mutations in the SARS-CoV-2 spike (S) gene. This assay targets the L452R, E484K/Q/A, and N501Y mutations, at least one of which is found in nearly all major variants. In a comparison of three different Cas12 enzymes, only the newly identified enzyme CasDx1 was able to accurately identify all targeted SNP mutations. An analysis pipeline for CRISPR-based SNP identification from 261 clinical samples yielded a SNP concordance of 97.3% and agreement of 98.9% (258 of 261) for SARS-CoV-2 lineage classification, using SARS-CoV-2 whole-genome sequencing and/or real-time RT-PCR as test comparators. We also showed that detection of the single E484A mutation was necessary and sufficient to accurately identify Omicron from other major circulating variants in patient samples. These findings demonstrate the utility of CRISPR-based DETECTR as a faster and simpler diagnostic method compared with sequencing for SARS-CoV-2 variant identification in clinical and public health laboratories.

KEYWORDS COVID-19, CRISPR-Cas12, DETECTR, LAMP, SARS coronavirus 2, SARS-CoV-2, assay validation, guide RNAs, variant, viral mutations

The emergence of new SARS-CoV-2 variants threatens to substantially prolong the COVID-19 pandemic. SARS-CoV-2 variants, especially variants of concern (VOCs) (1, 2), have caused resurgent COVID-19 outbreaks in the United States (2–5) and worldwide (1, 6, 7), even in populations with a high proportion of vaccinated individuals (8–11). Mutations in the spike protein, which binds to the human ACE2 receptor, can render the virus more infectious and/or more resistant to antibody neutralization, resulting in increased transmissibility (12), and/or escape from immunity, whether vaccine-mediated or naturally acquired immunity (13, 14). Variant identification can also be clinically significant, as some mutations substantially reduce the effectiveness of available monoclonal antibody therapies for the disease (15).

Tracking the evolution and spread of SARS-CoV-2 variants in the community can inform public policy regarding testing and vaccination, as well as guide contact tracing and containment effects during local outbreaks (16, 17). Virus whole-genome sequencing (WGS) and single nucleotide polymorphism (SNP) genotyping are commonly used

Editor Melissa B. Miller, UNC School of Medicine

Copyright © 2022 American Society for Microbiology. All Rights Reserved.

Address correspondence to Janice S. Chen, janice@mammoth.bio, or Charles Y. Chiu, Charles.Chiu@ucsf.edu.

The authors declare a conflict of interest. C.Y.C. is the director of the UCSF-Abbott Viral Diagnostics and Discovery Center and receives research support from Abbott Laboratories, Inc. C.L.F., B.M., V.N., J.P.B., R.N.D., E.S., C.G.H., J.C., and J.S.C. are employees of Mammoth Biosciences. C.Y.C. is a member of the scientific advisory board for Mammoth Biosciences. The other authors declare no competing interests.

Received 17 February 2022

Returned for modification 21 March 2022

Accepted 1 June 2022

Published 29 June 2022

to identify variants (16, 18), but can be limited by long turnaround times and/or the requirement for bulky and expensive laboratory instrumentation. Diagnostic assays based on clustered interspaced short palindromic repeats (CRISPR) (19) have been developed for rapid detection of SARS-CoV-2 in clinical samples (13, 20–23), and a few have obtained emergency use authorization (EUA) by the U.S. Food and Drug Administration (FDA) (24–26). Some advantages of these assays for use in laboratory and point-of-care settings include low cost, minimal instrumentation, and a sample-to-answer turnaround time of under 2 h (20, 23, 27–29).

Here, we present the development of a CRISPR-based COVID-19 variant DETECTR assay (henceforth abbreviated as DETECTR assay) for the detection of SARS-CoV-2 mutations and evaluate its performance on a total of 304 patient respiratory swab samples using WGS as a comparator method (Fig. 1A). The assay combines RT-LAMP pre-amplification followed by fluorescent detection using a CRISPR-Cas12 enzyme. We perform a comparative evaluation of multiple candidate Cas12 enzymes and demonstrate that robust assay performance depends on the specificity of the newly identified CRISPR-Cas12 enzyme called CasDx1 in identifying key SNP mutations of functional relevance in the spike protein at amino acid positions 452, 484, and 501 (30).

MATERIALS AND METHODS

Synthetic gene fragments. Wild-type (WT) and mutant (MUT) synthetic gene fragments (Twist) were PCR amplified using NEB 2x Phusion Master Mix following the manufacturer's protocol. The amplified product was cleaned using AMPure XP beads following manufacturer's protocol at a 0.7x concentration. The product was eluted in nuclease-free water and normalized to 10 nM. All nucleic acids used in this study are summarized in Data set S3.

Clinical sample acquisition and extraction. De-identified residual SARS-CoV-2 RT-PCR positive nasopharyngeal and/or oropharyngeal (NP/OP) swab samples in universal transport media (UTM) or viral transport media (VTM) were obtained from the UCSF Clinical Microbiology Laboratory. All samples were stored at -80°C in a biorepository according to protocols approved by the UCSF Institutional Review Board (protocol number 10-01116, 11-05519) until processed.

All NP/OP swab samples obtained from the UCSF Clinical Microbiology Laboratory were pretreated with DNA/RNA Shield (Zymo Research, # R1100-250) at a 1:1 ratio. The Mag-Bind Viral DNA/RNA 96 kit (Omega Bio-Tek, # M6246-03) on the KingFisher Flex (Thermo Fisher Scientific, # 5400630) was used for viral RNA extraction using an input volume of 200 μL of diluted NP/OP swab sample and an elution volume of 100 μL . The Taqpath COVID-19 RT-PCR kit (Thermo Fisher Scientific) was used to determine the N gene cycle threshold values.

Heat-inactivated culture acquisition and extraction. Heat-inactivated cultures of SARS-CoV-2 variants being monitored (VBM), VOC, or variants of interest (VOI) were provided by the California Department of Public Health (CDPH). RNA from heat-inactivated SARS-CoV-2 VBM/VOC/VOI isolates were extracted using the EZ1 Virus minikit v2.0 (Qiagen, # 955134) on the EZ1 Advanced XL (Qiagen, # 9001875) according to the manufacturer's instructions. For each culture, six replicate LAMP reactions were pooled into a single sample. DETECTR was performed on a 1:10 dilution of the 10,000 cp/rxn LAMP amplification products.

COVID-19 variant DETECTR assay. Two LAMP primer sets, each containing six primers, were designed to target the L452R, E484K, and N501Y mutations in the SARS-CoV-2 Spike (S) protein (Data set S3). Sets of LAMP primers were designed from a 350-bp target sequence spanning the three mutations using Primer Explorer V5 (<https://primerexplorer.jp/e/>). Candidate primers were manually evaluated for inclusion using the OligoCalc online oligonucleotide properties calculator (31) while ensuring that there was no overlap with either primers from the other set or guide RNA target regions that included the L452R, E484K, and N501Y mutations.

Multiplexed RT-LAMP was performed using a final reaction volume of 50 μL , which consisted of 8 μL RNA template, 5 μL of L452R primer set (Eurofins Genomics), 5 μL of E484K/N501Y primer set, 17 μL of nuclease-free water, 1 μL of SYTO-9 dye (Thermo Fisher Scientific), and 14 μL of LAMP mastermix. Each of the primer sets consisted of 1.6 μM (each) inner primers FIP and BIP, 0.2 μM (each) outer primers F3 and B3, and 0.8 μM (each) loop primers LF and LB. The LAMP mastermix contained 6 mM MgSO_4 , isothermal amplification buffer at 1X final concentration, 1.5 mM dNTP mix (NEB), 8 units of Bst 2.0 WarmStart DNA polymerase (NEB), and 0.5 μL of WarmStart RTx Reverse Transcriptase (NEB). Plates were incubated at 65°C for 40 min in a real-time Quantstudio 5 PCR instrument. Fluorescent signals were collected every 60 s.

Degenerate multiplexed RT-LAMP was performed using a final reaction volume of 65 μL , which consisted of 9.6 μL RNA template, 10 μL of L452R degenerate primer set (Eurofins Genomics), 10 μL of E484K/N501Y degenerate primer set, 14.1 μL of nuclease-free water, 1.3 μL of SYTO-9 dye (Thermo Fisher Scientific), and 20 μL of LAMP mastermix. The primer set and mastermix assembly, the incubation, and data collection were described above.

A concentration of 40 nM CasDx1 (Mammoth Biosciences), LbCas12a (EnGen Lba Cas12a, NEB) or AsCas12a (Alt-R A.s. Cas12a, IDT) protein targeting the WT or MUT SNP at L452 (R), E484 (K) or N501 (Y) was incubated with 40 nM gRNA in 1X buffer (MBuffer3 for CasDx1, NEBuffer r2.1 for LbCas12a and

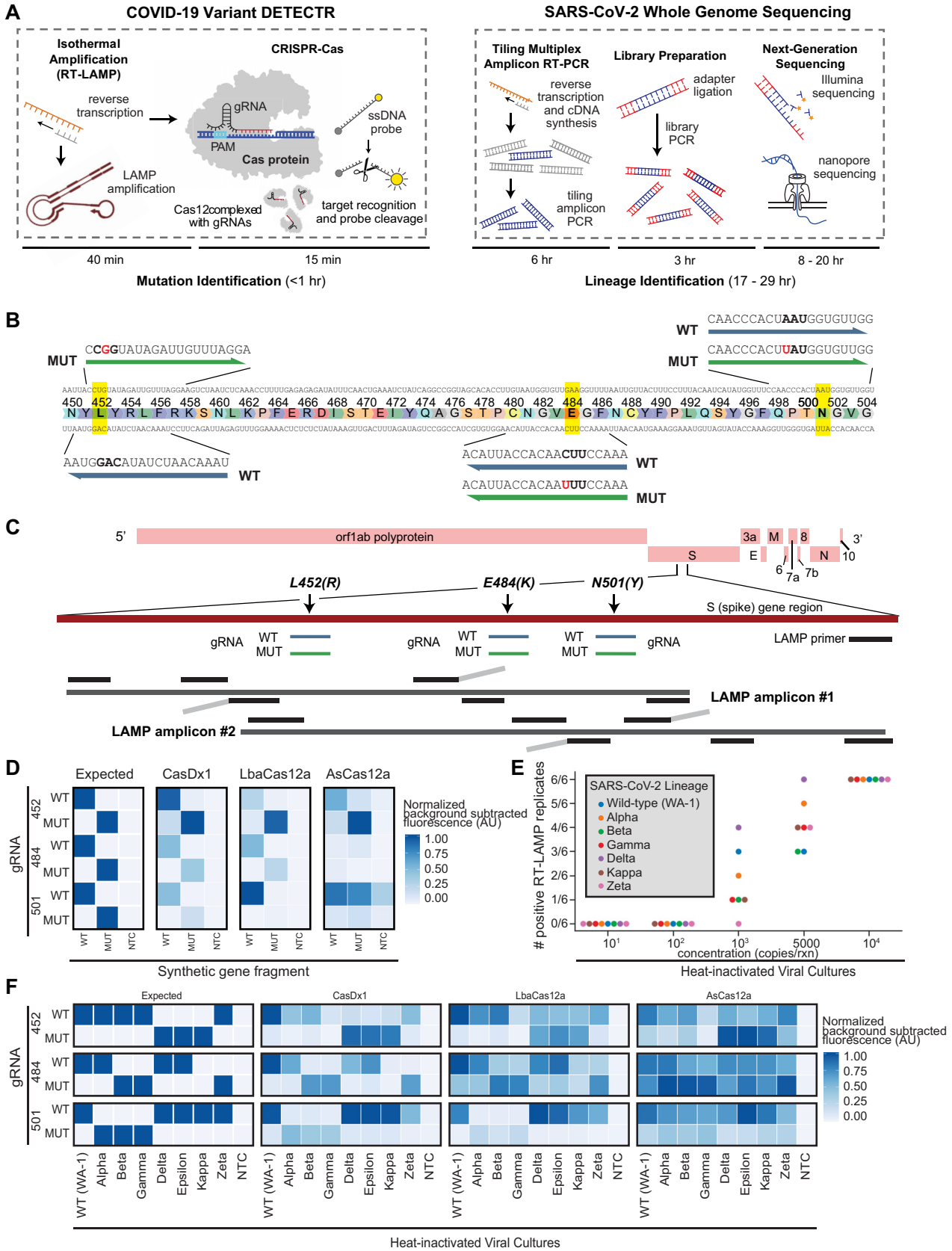


FIG 1 Design and workflow for the DETECTR assay. (A) Workflow comparison between the DETECTR assay and SARS-CoV-2 whole-genome sequencing (WGS) using either Illumina benchtop or Oxford Nanopore Technologies (ONT) nanopore sequencers. (B) Schematic of CRISPR-Cas gRNA (Continued on next page)

AsCas12a) for 30 min at 37°C. CasDx1 gRNAs were used with both CasDx1 and LbCas12a, whereas AsCas12a gRNAs were used with AsCas12a (Data set S3). Then, 100 nM ssDNA reporter (5'Alex594N/TTATTATT/3IAbrQSp/, IDT) was added to the RNA-protein complex; 18 µL of this DETECTR master mix was combined with 2 µL target amplicon. The DETECTR assays were monitored for 30 min at 37°C in a plate reader (Tecan).

Digital PCR. Samples were evaluated at three dilutions (1:100; 1:1,000; and 1:10,000) using the ApexBio Covid-19 Multiplex Digital PCR Detection Kit (Stilla Technologies) according to the manufacturer's protocol. The controls (positive and negative provided by UCSF, the Kit Controls, and an internal control) were run with the samples in duplicate. The dilutions were used to determine the most accurate concentration which was determined from the N gene concentration.

Sequencing methods. Complementary DNA (cDNA) synthesis from RNA via reverse transcription and tiling multiplexed amplicon PCR were performed using SARS-CoV-2 primers version 3 according to the ARTIC protocol (32, 33). Libraries were constructed by ligating adapters to the amplicon products using NEBNext Ultra II DNA Library Prep Kit for Illumina (New England Biolabs, # E7645L), barcoding using NEBNext Multiplex Oligos for Illumina (New England Biolabs, # E6440L), and purification with AMPure XP (Beckman-Coulter, # 63880). Final pooled libraries were sequenced on either Illumina MiSeq or NextSeq 550 as 2 × 150 single-end reads (300 cycles).

SARS-CoV-2 viral genome assembly and variant analyses were performed using an in-house bioinformatics pipeline. Briefly, sequencing reads generated by Illumina sequencers (MiSeq or NextSeq 550) were demultiplexed and converted to FASTQ files using bcl2fastq (v2.20.0.422). Raw FASTQ files were first screened for SARS-CoV-2 sequences using BLASTn (BLAST+ package 2.9.0) alignment against the Wuhan-Hu-1 SARS-CoV-2 viral reference genome (NC_045512). Reads containing adapters, the ARTIC primer sequences, and low-quality reads were filtered using BBDuk (version 38.87) and then mapped to the NC_045512 reference genome using BBDuk (version 38.87). Variants were called with CallVariants and iVar (version 1.3.1) and a depth cutoff of 5 was used to generate the final assembly. Pangolin software (version 3.1.17) (34, 35) was used to identify the lineage. Using a custom in-house script, consensus FASTA files generated by the genome assembly pipeline were scanned to confirm L452R, E484K, and N501Y mutations.

Discordant sample retesting. Discordant samples ($n = 16$) stored at -80°C were re-extracted as described above for the NP/OP swab samples and evaluated by viral WGS as described above. The extracted nucleic acids were then thawed (incurring an additional freeze/thaw as needed) and amplified using the LAMP protocol described above and evaluated using the DETECTR assay as described above.

Discrepancy testing using the Simplexa SARS-CoV-2 variants assay. Six discordant samples and 14 concordant samples were evaluated from the initial extracts using the manufacturer's instructions for the Simplexa SARS-CoV-2 Variants (DiaSorin). In brief, 50 µL reaction mixture was loaded into the reaction (R) well and 50 µL of sample or control was loaded into the "SAMPLE" well. Adhesive foil cover sealed the "direct amplification disc" which was loaded into the LIAISON MDX and run.

DETECTR data analysis pipeline. (i) Quality control metrics for the LAMP reaction. Prior to processing DETECTR data from the clinical samples, we collected data indicating the success or failure of the samples to amplify in the LAMP reaction. The absolute truth was based on visual inspection of LAMP curves. This absolute truth was used to develop thresholds for the LAMP reactions. The positive and negative controls from the LAMP reactions were used to derive the thresholds to qualify the samples. Two sets of thresholds were used: time threshold and fluorescence rate threshold. The positive LAMP controls were assumed to represent an ideal sample and displayed a classic sigmoidal rise of fluorescence over time and the NTC represented the background fluorescence. It was hypothesized that a sample would ideally have positive control like fluorescence kinetics. However, due to the presence of high background in some samples, a mean value between controls for each plate was chosen as threshold. After this, the fluorescence values at a time threshold of 18 min were collected in order to rule out those samples that would amplify closer to the endpoint, signifying the LAMP intermediates to be the majority contributors of the rise in the signal and not the actual sample itself. A score was assigned for each sample which was calculated as a ratio of rate of fluorescence rate threshold to the rate of fluorescence value at 18 min for each sample. To identify the exact score value for a qualitative QC metric, an ROC analysis was done on scores and the absolute truth and Youden's index was determined.

(ii) Data analysis for CRISPR-based SNP calling. Each well had a guide specific to the mutant or the WT SNP to assign a genotypic call to the sample. As the DETECTR reactions across the plate were not comparable to each other, the endpoint fluorescence intensities were normalized in each well to its own minimum intensity (fluorescence yield). The fluorescence yield was compared across wells in a plate under the assumption that each well would have similar minimum fluorescence starting point. Irrespective of the highest levels of the fluorescence intensities observed across samples, the yield for a given target remained the same assuming that similar concentrations of samples and target were being compared. This aided in normalizing the signal and comparing replicates across the wells in the same plate.

$$F_y = \max(F) / \min(F)$$

FIG 1 Legend (Continued)

design for SARS-CoV-2 S gene mutations. (C) Schematic of multiplexed RT-LAMP primer design showing a map of the positions of the SARS-CoV-2 S gene mutations (arrows), primers (black; black-gray), and gRNAs (blue for WT, green for MUT) within the S-gene target region. (D) Heat map comparison of three different Cas12 enzymes tested using 10 nM PCR-amplified synthetic gene fragments ($t = 30$ min). (E) Dot plot showing the number ($n = 6$) of positive RT-LAMP replicates from heat-inactivated viral cultures corresponding to known variants across a 4-log dynamic range. (F) Heat map comparison of endpoint fluorescence ($t = 30$ min) of three different Cas12 enzymes tested against heat-inactivated viral cultures.

The intensities of the WT and mutant target guides on NTC were assumed to remain constant over time. The fluorescence yield for NTC was also assumed to remain constant across replicates and plates and be close to 1. The zone of fluorescence yield for a plate was dependent on the number of NTCs included in the experiment, as follows:

$$F_y(NTC) = 1 \text{ (theoretically)}$$

$$F_y(NTC) = [0.5, 1.7] \text{ (observed range)}$$

A sample with a fluorescence yield of 1 was assigned a “no call.” Contrast and size were calculated for the fluorescence data and used for comparing the signals. Contrast was calculated as log difference between the WT and MUT signals and size as the mean average of the logarithm of the signals between WT and MUT guides. The contrast value for NTC was expected to hover around 0 and average signal strength (size) for NTC very low compared to the samples. The contrast values aided in the identification of the WT or MUT in addition to ruling out low signal or noise from the NTC.

(iii) General rules for variant calling.

1. NTC was assigned NTC.
2. If the contrast of the sample for a SNP was between minimum and maximum contrast for the plate, then the sample was assigned a no call.
3. If the size of the sample was lower than the size of the NTC on the plate, then the sample was assigned a no call.

$$C_{min}(NTC-snp) \leq C(\text{sample-snp}) \leq C_{max}(NTC-snp) \rightarrow \text{NoCall}$$

$$S_{min}(NTC-snp) \leq S(\text{sample-snp}) \leq S_{max}(NTC-snp) \rightarrow \text{NoCall}$$

$$\log_2(F_y(WT)) > \log_2(F_y(M)) \rightarrow \text{Wild Type}$$

$$\log_2(F_y(WT)) < \log_2(F_y(M)) \rightarrow \text{Mutant}$$

In cases where more than one mutant at a particular position was being analyzed for, then signals of each mutant were compared with the WT signal. If there existed a mutant, then among (n) comparisons for n mutants and one WT, one of the comparisons would be expected to yield a mutant call.

$$\log_2(F_y(WT)) > \log_2(F_y(M1)) \rightarrow \text{Wild Type}$$

$$\log_2(F_y(WT)) > \log_2(F_y(M2)) \rightarrow \text{Wild Type}$$

$$\log_2(F_y(WT)) > \log_2(F_y(M3)) \rightarrow \text{Wild Type}$$

$$\log_2(F_y(WT)) < \log_2(F_y(M4)) \rightarrow \text{Mutant (4)}$$

If there was a tie in the above logic between mutant and WT, then a tie breaker comparison would yield a final result.

$$\log_2(F_y(WT)) > \log_2(F_y(M1)) \rightarrow \text{Wild Type}$$

$$\log_2(F_y(WT)) < \log_2(F_y(M2)) \rightarrow \text{Mutant (2)}$$

$$\log_2(F_y(WT)) > \log_2(F_y(M3)) \rightarrow \text{Wild Type}$$

$$\log_2(F_y(WT)) < \log_2(F_y(M4)) \rightarrow \text{Mutant (4)}$$

$$\log_2(F_y(M2)) < \log_2(F_y(M4)) \rightarrow \text{Mutant (4)}$$

(iv) SNP calls. We used the following procedure to evaluate the concordance between sequencing and DETECTR technologies for genotypic classification of the clinical cohort data set. First, we considered all samples and SNPs for which both sequencing and DETECTR data were present in the distributed files by matching the SNP IDs and sample names. This included cleaning and curing the data set which had failed LAMP reactions and identifying WT and MUT based on the spacer fluorescent. This yielded a preliminary data set containing 279 calls across three SNPs against 93 samples. After eliminating samples that failed to amplify in the LAMP reaction but were assigned a genotype, the resulting final analysis

data consisted of 272 calls (WT, MUT, and no call) spread across three SNPs and 91 samples. For each of the three SNPs in the analysis data set, we identified and recorded both sequencing and DETECTR genotypes (including no calls and LAMP fails) for each of the 93 patients. The 91 patients included individuals for whom actual sequencing data were available.

Statistical analysis. For each SNP in the analysis, we computed a variety of statistics evaluating the concordance between genotype calls on the two different technologies. The concordant and discordant genotypes were visualized through contingency tables. For each SNP, there are three possible genotypes (WT, MUT, and no call). The concordance rates were calculated without the samples that failed the LAMP reaction. The 2×2 cross tables classify all three SNPs across all the samples between sequencing and DETECTR technologies. The data transformation and statistical analysis was done using the R software package (36).

Ethical statement. We confirm all relevant ethical guidelines have been followed, and any necessary IRB and/or ethics committee approvals have been obtained.

Data availability. All data needed to evaluate the conclusions in the paper are present in the paper and/or the supplementary materials. The CasDx1 protein can be provided by Mammoth Biosciences to the extent feasible, pending scientific review and a completed material transfer agreement. Requests for the CasDx1 protein should be submitted to Janice Chen at janice@mammothbiosci.com.

RESULTS

Identifying the optimal CRISPR-Cas12 enzyme for SNP detection. To determine the optimal Cas12 enzyme for SNP detection, we evaluated three different CRISPR-Cas effectors with transcutting activity: LbCas12a, AsCas12a, and a novel Cas12 enzyme called CasDx1. We initially screened guide RNAs (gRNAs) with CasDx1 and LbCas12a for activity on synthetic gene fragments encoding regions of the SARS-CoV-2 S-gene with either WT or MUT sequences at amino acid positions 452, 484, and 501 (Fig. 1B, C). From this initial activity screen, we identified the top-performing gRNAs for each S-gene variant encoding either L452R, E484K or N501Y (Fig. 1D). Further evaluation of these guides using CasDx1, LbCas12a, and AsCas12a with their cognate gRNAs on synthetic gene fragments revealed differences in SNP differentiation capabilities, with CasDx1 showing the clearest SNP differentiation between WT and MUT sequences for all targeted S-gene variants (Fig. 1D; Fig. S1A). In comparison, LbCas12a could differentiate SNPs at positions 452 and 484, but not 501, whereas AsCas12a could only differentiate the SNP at position 452 (Fig. 1D; Fig. S1A).

We next tested SNP differentiation capabilities on heat-inactivated viral cultures using the full DETECTR assay, consisting of RNA extraction, multiplexed RT-LAMP amplification (Fig. 1C), and CRISPR-Cas12 detection with guide RNAs targeting part of the spike receptor-binding domain (RBD) (Fig. 1B). The LAMP primer design incorporated two sets of six primers each, with both sets generating overlapping spike RBD amplicons that spanned the L452R, E484K, and N501Y mutations. We chose to adopt a redundant LAMP design for two reasons: first, this approach was shown to improve detection sensitivity in initial experiments; second, we sought to increase assay robustness given the continual emergence of escape mutations in the spike RBD throughout the course of the pandemic (13). Inclusivity analysis using representative sequences from the Alpha, Beta, Gamma, and Delta variants revealed that $\geq 91.7\%$ and $\geq 99\%$ of viruses would have ≤ 1 and ≤ 2 nucleotide mismatches in the LAMP primers, respectively (Data set S1). The tested viral cultures included an ancestral SARS-CoV-2 lineage (WA-1) containing the WT spike protein (D614) targeted by the approved mRNA (BNT162b2 from Pfizer or mRNA-1273 from Moderna) (37, 38) and DNA adenovirus vector (Ad26.COVS from Johnson and Johnson) (39) vaccines, VBMs that were previously classified as VOCs or VOIs, including Alpha (B.1.1.7), Beta (B.1.351), Gamma (P.1), Epsilon (B.1.427 and B.1.429), Kappa (B.1.617.1), and Zeta (P.2) lineages, and the current VOC Delta (B.1.617.2) lineage (40). Heat-inactivated viral culture samples representing the seven SARS-CoV-2 lineages were quantified by digital droplet PCR across a 4-log dynamic range and used to evaluate the analytical sensitivity of the pre-amplification step. RT-LAMP amplification was evaluated using six replicates from each viral culture. We observed successful amplification for each of the seven representative SARS-CoV-2 lineages at a concentration of 2×10^5 copies/mL (10,000 copies/reaction) (Fig. 1E), comparable with the range of concentrations ($> 2 \times 10^5$ copies/mL, or < 30 Ct value) required for sequencing workflows used in SARS-CoV-2 variant surveillance (41, 42).

To evaluate the specificity of the different Cas12 enzymes, amplified material from each viral culture was pooled and the SNPs resulting in the L452R, E484K, and N501Y mutations were detected using CasDx1, LbCa12a, and AsCas12a. Similar to the results found using gene fragments, CasDx1 correctly identified the WT and MUT targets at positions 452, 484, and 501 in each LAMP-amplified, heat-inactivated viral culture (Fig. 1F; Fig. S1B). In comparison, LbCas12a could differentiate WT from MUT at position 501 on LAMP-amplified viral cultures but showed much higher background for the WT target at position 452 and higher background for both WT and MUT targets at position 484 for (Fig. 1F; Fig. S1B). Additionally, AsCas12a could differentiate WT from MUT targets at position 452, albeit with substantial background but was unable to differentiate WT from MUT targets at positions 484 and 501 (Fig. 1F; Fig. S1B). From these data, we concluded that CasDx1 would provide more consistent and accurate calls for the L452R, E484K, and N501Y mutations. We thus proceeded to further develop the assay using only the high-fidelity CasDx1 enzyme.

Data analysis pipeline for calling COVID-19 variant SNPs with the DETECTR assay. To develop a data analysis pipeline for calling SARS-CoV-2 SNP mutations and assign lineage classifications with the DETECTR assay (Fig. 2A, B), we first used data collected from SNP synthetic gene fragment controls ($n = 279$) that included all mutational combinations of 452, 484 and 501 (see Materials and Methods). Based on the control sample data, we generated allele discrimination plots (43, 44) to define boundaries that separated the WT and MUT signals (Fig. S2A). Clear differentiation between WT and MUT signals was observed when plotting the ratio against the average of the WT and MUT transformed values on a mean average (MA) plot (43, 44) (Fig. S2B), with 100% concordance for SNP identity at positions 452, 484, and 501 for the control samples.

Performance evaluation of the DETECTR assay using clinical samples. Next, we assembled a blinded data set consisting of 93 COVID-19 positive clinical samples (previously analyzed by viral WGS) and the SNP controls run in parallel. These samples were extracted, amplified in triplicate RT-LAMP reactions (Fig. S3A), and processed further as triplicate CasDx1 reactions for each LAMP replicate (Fig. S3B). A total of nine replicates were thus generated for each sample to detect WT or MUT SNPs at positions 452, 484, and 501. This experimental design provided sufficient data points (control and experimental) from which to refine the data analysis pipeline. The DETECTR data analysis pipeline was then applied to each sample to provide a final lineage categorization (Fig. 2A to C). For a biological RT-LAMP replicate to be designated either WT or MUT, the same call needed to be made from all three technical CasDx1 replicates (Fig. S4A). If the three RT-LAMP biological replicates resulted in different calls, a “no call” was assigned to the sample and it was reflexed to retesting. A final SNP mutation call was made based on ≥ 1 of the same calls from the three RT-LAMP biological replicates, with replicates that were designated a no call ignored (Fig. S4A to C). After excluding two samples that were considered invalid because the fluorescence intensity from RT-LAMP amplification did not reach a pre-established threshold determined using receiver-operator characteristic (ROC) curve analysis (Fig. S3A), we evaluated a total of 807 CasDx1 signals from the 91 remaining clinical samples, generating up to nine replicates for each clinical sample (Fig. S4B). Differentiation of WT and MUT signals according to the allele discrimination plots was more pronounced at positions 484 and 501 than position 452 (Fig. S3), whereas the MA plots, generated by transforming the data onto M (log ratio) and A (mean average) scales, showed clear separation of WT and MUT calls for all three positions (Fig. 3A; Fig. S2). The variant calls made on each sample were consistent with the difference in median values of the log-transformed signals as determined using the data analysis pipeline (Fig. S5).

We then unblinded the viral WGS results to evaluate the accuracy of the DETECTR assay for SNP calls and lineage classification. There were 14 discordant SNP calls out of 272 (94.9% SNP concordance) distributed among 11 clinical samples out of 91 (Fig. S6A to C). Among the 11 discordant samples, one sample (COVID-31) was designated a no call at position 452 by viral WGS and thus lacked a comparator, two samples were

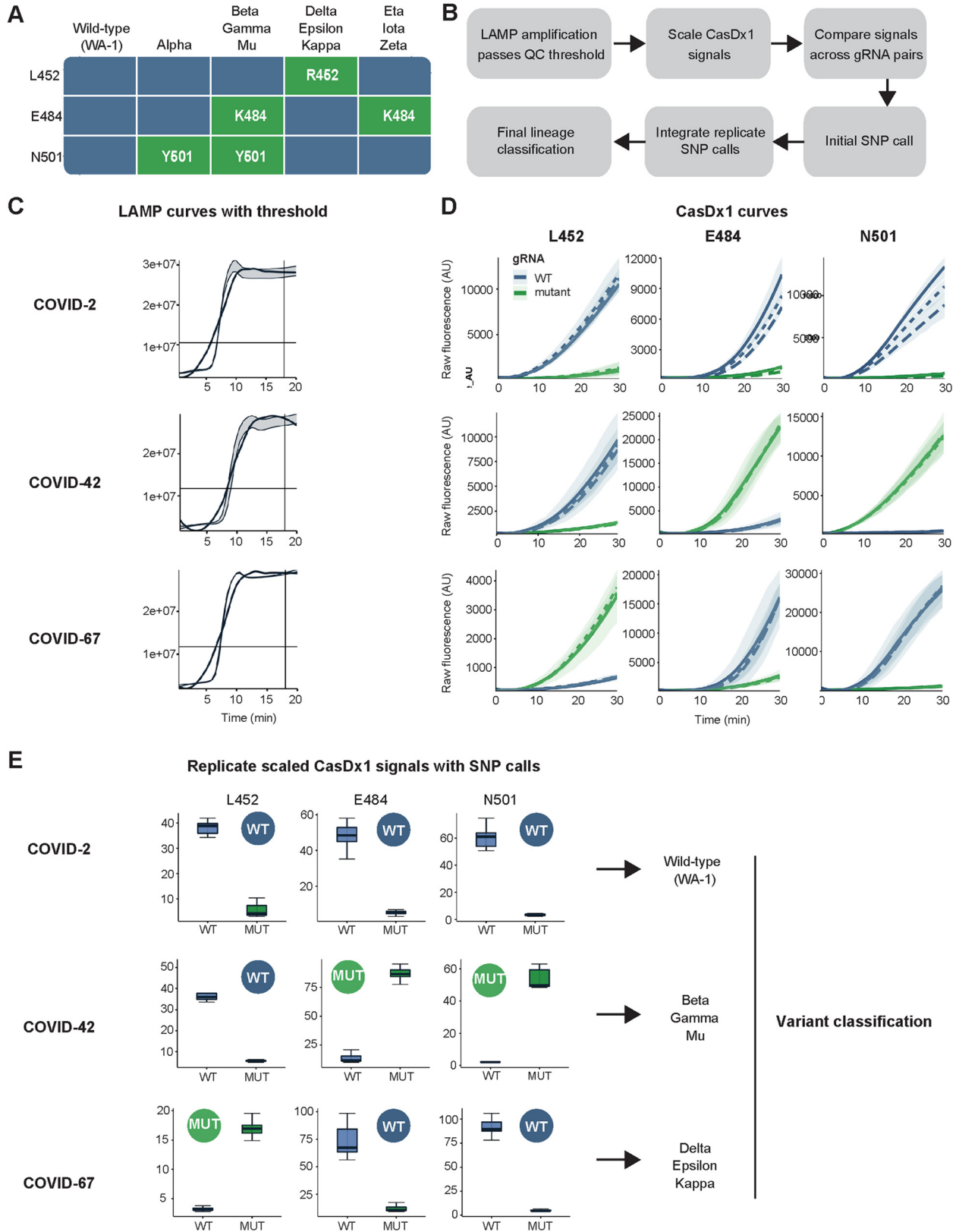


FIG 2 DETECTR data analysis pipeline for SARS-CoV-2 SNP mutation calling. (A) Interpretation table summarizing the SARS-CoV-2 mutations in this study associated with corresponding lineage classifications. (B) Flow chart of the lineage classification algorithm. Scaled signals are compared across SNPs and calls are made for each RT-LAMP replicate. The combined replicate calls defines the mutation call, which informs the final lineage classification. (C, D, and E) Three representative clinical samples of different SARS-CoV-2 lineages to demonstrate the workflow of the DETECTR assay.

(Continued on next page)

designated a no call due to flat WT and MUT curves (COVID-41 and COVID-73), four samples had similar WT and MUT curve amplitudes, suggesting a mixed population (COVID-03, COVID-56, COVID-61, and COVID-81) (Fig. S6A), and four samples had SNP assignments discordant with those from viral WGS (COVID-12, COVID-13, COVID-20, and COVID-63) (Fig. S6A).

Given that the comparison data had been collected over an extended time period, we surmised that sample stability issues arising from aliquoting and multiple freeze-thaw cycles may have accounted for the observed discrepancies. To further investigate this possibility, the 11 discordant clinical samples were re-extracted from the original respiratory swab matrix and re-analyzed by running both viral WGS and the DETECTR assay in parallel. Retesting of the samples resulted in nearly complete agreement between the two methods, except for two SNPs that were identified as E484Q in two samples by WGS but were incorrectly called E484 (WT) by the DETECTR assay (Fig. 3B, C). Thus, based on discrepancy testing, the positive predictive agreement (PPA) between the DETECTR assay and viral WGS at all three WT and MUT SNP positions was 100% (272 of 272) (Fig. 3D). The corresponding negative predictive agreement (NPA) at position 484 was 91.3% as the E484Q mutation for two SNPs was incorrectly classified as WT. Nevertheless, the final viral lineage classification for the 91 samples after discrepancy testing showed 100% agreement ($P < 2.2e-16$ by Fisher's exact test) with viral WGS (Fig. 3C; Data set S2).

In November 2021, a new SARS-CoV-2 variant, called Omicron, was identified and almost immediately designated a variant of concern (45). The Omicron variant carries an exceptionally high number of mutations (>30) within the S-gene and has been shown to have enhanced transmissibility and immune evasion (46, 47). The record number of COVID-19 cases globally from Omicron and loss of activity by certain therapeutic antibodies underscores the need for rapid and targeted identification of SARS-CoV-2 variants. Although the TaqPath PCR assay with S-gene target failure (SGTF) has functioned as a screen that can be reflexed to sequencing to identify the Omicron variant (48), the SGTF assay alone cannot differentiate between Omicron BA.1 and Alpha (49, 50) and cannot identify emerging Omicron variants that lack the SGTF, such as the BA.2 sublineage (49). We, therefore, quickly reconfigured our COVID-19 variant DETECTR assay for the identification of Omicron by targeting the E484A mutation, which alone differentiates Omicron from all other current VBM/VOI/VOC. Given that E484-related mutations are present in multiple circulating variants and have a strong effect on reducing antibody neutralization (10, 51, 52), we further updated our panel of CasDx1 gRNAs to detect all relevant mutations (E, K, Q, and A) at amino acid position 484 (Fig. 4A, B).

Given the highly mutated Omicron S-gene, we suspected that our original LAMP primer set would not have sufficient sensitivity to amplify the targeted spike RGD region, and thus, we incorporated degenerate nucleotides within the LAMP primers to enable amplification of the Omicron S-gene (Fig. 4A; Data set S3). Inclusivity analysis using representative sequences from the Alpha, Beta, Gamma, Delta, and Omicron variants revealed that $\geq 98.1\%$ and $\geq 99.4\%$ of viruses would have ≤ 1 and ≤ 2 nucleotide mismatches in the degenerate LAMP primers, respectively (Data set S1). Within weeks of the first Omicron case identified in the United States. (53), we procured and tested an additional set of 48 clinical samples. These samples were blinded and processed with the updated DETECTR assay workflow, which included sample extraction, followed by amplification with the degenerate LAMP primers and detection with each of the 484-specific CasDx1 gRNAs. Once processed, a result with mutations K484, Q484,

FIG 2 Legend (Continued)

(C) Raw fluorescence curves of each sample run in RT-LAMP amplification. (D) Subsequent triplicate DETECTR reactions targeting both WT and MUT SNPs for L452 (R), E484 (K), and N501 (Y). (E) Box plot visualization of the endpoint fluorescence in DETECTR across each SNP for the three representative clinical samples. Calls of WT, MUT, or no call were made for each SNP by evaluating the median values of the DETECTR calls corresponding to LAMP replicates. Final calls are made on the lineage determined by each SNP. Blue represents WT and green represents MUT, with RT-LAMP replicates ($n = 3$), CasDx1 replicates ($n = 3$ per LAMP replicate), and shading around kinetic curves indicates ± 1.0 SD.

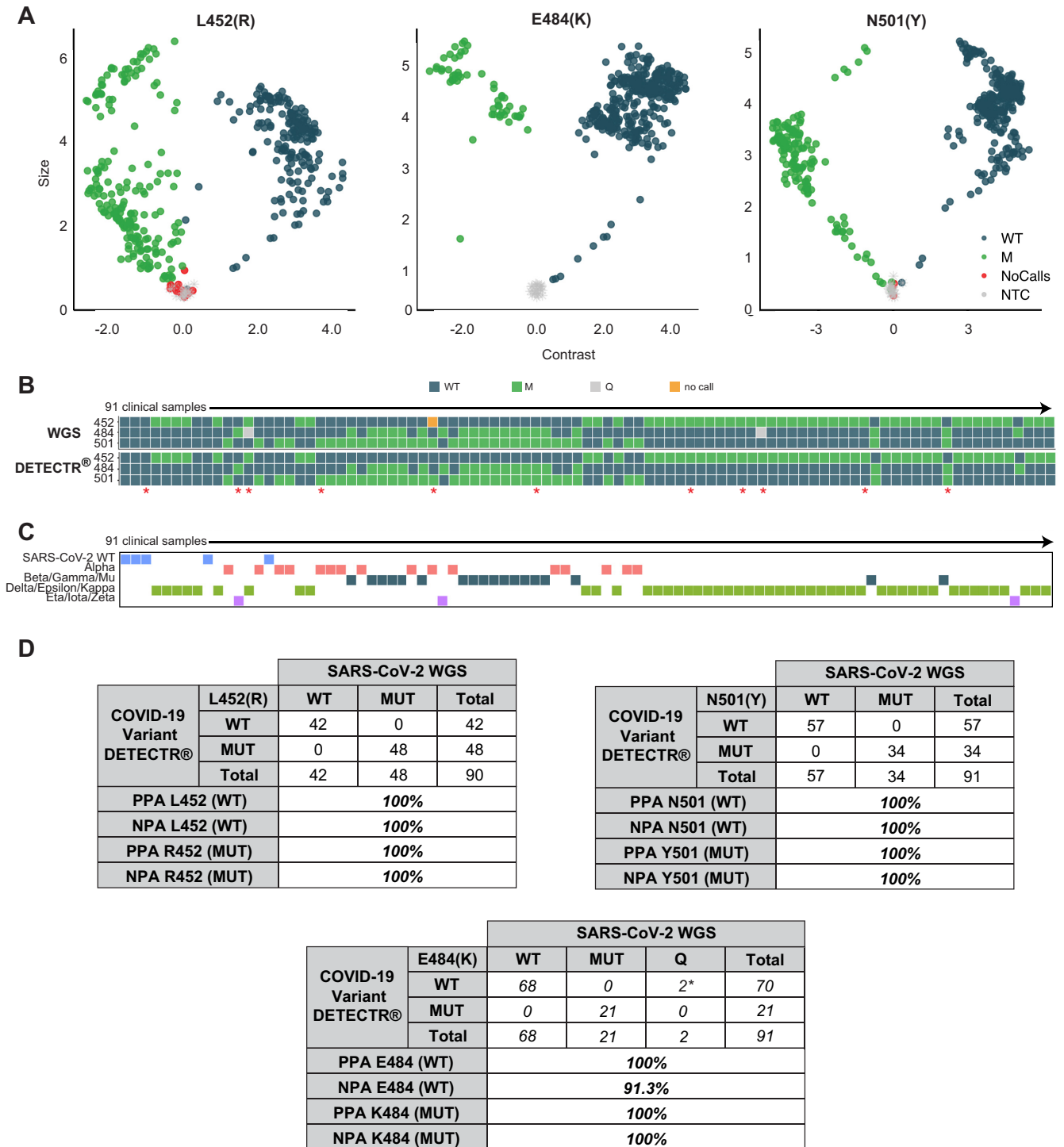
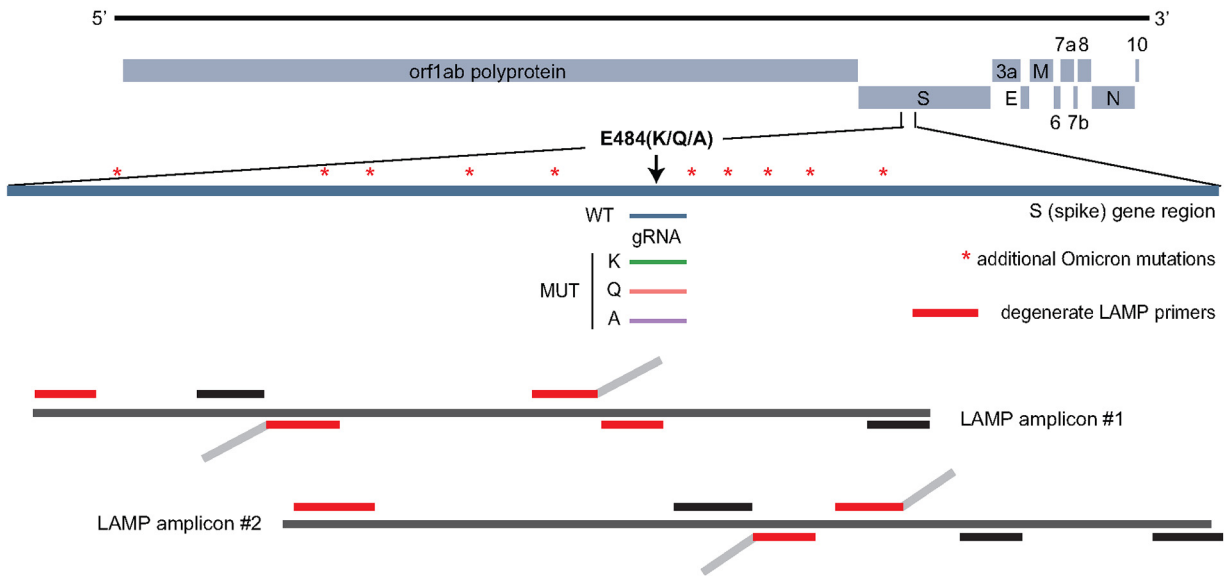
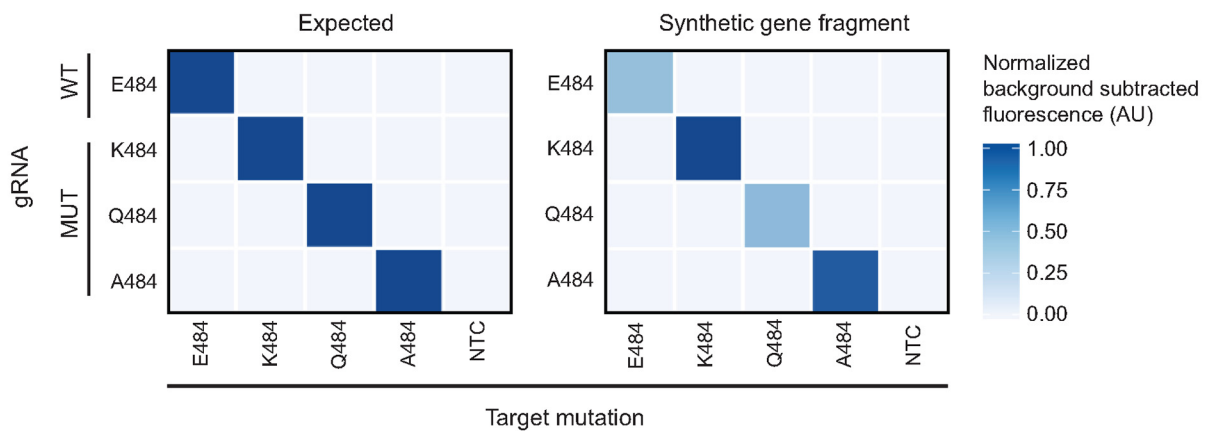


FIG 3 Comparison of the DETECTR assay to SARS-CoV-2 whole-genome sequencing. (A) MA plots, transformed into M (log ratio) and A (mean average) scales, show CasDx1 SNP detection replicates ($n = 807$) for each SARS-CoV-2 mutation across 91 clinical samples. WT is denoted by blue dots, MUT is denoted by green dots, no call is denoted by orange dots and NTC is denoted by gray dots. (B) Alignment of final mutation calls comparing the DETECTR and SARS-CoV-2 WGS assay results across 91 clinical samples after discordant samples (indicated by red asterisk) were resolved. (C) Final lineage classification on each clinical sample by the DETECTR assay compared to the SARS-CoV-2 lineage determined by viral WGS. Lineage classification categories include SARS-CoV-2 WT (blue), Alpha (red), Beta/Gamma/Mu (teal), Delta/Epsilon/Kappa (green), and Eta/Iota/Zeta (purple). (D) Final positive predictive agreement (PPA) and negative predictive agreement (NPA) values for each WT and MUT SNP from the evaluation of the DETECTR assay against the SARS-CoV-2 WGS comparator assay after discordant samples were resolved.

A



B



C



E

SNP	Concordance	p-value
E484	94.7%	<1.88E-15
K484	100%	<1.88E-15
Q484	100%	<1.88E-15
A484	100%	<1.88E-15

D

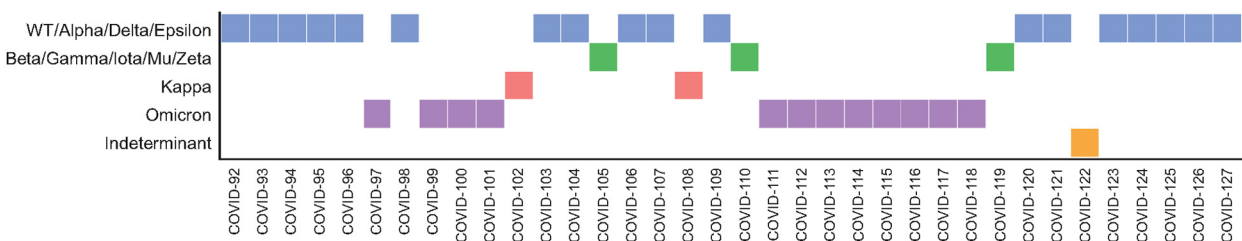


FIG 4 Specific detection of 484 mutations enables rapid Omicron identification. (A) Schematic of Omicron mutations within the S-gene LAMP amplicon and relative position of 484-specific gRNAs and degenerate LAMP primers. (B) Heat map comparison of endpoint fluorescence ($t = 30$ min) showing (Continued on next page)

or A484 was called Beta/Eta/Gamma/Iota/Mu/Zeta, Kappa, or Omicron, respectively (Fig. 4C to E; Fig. S7A). If the result was associated with E484 (WT), we ran the assay using WT and MUT gRNAs at positions 452 and 501 to call the final SARS-CoV-2 lineage (Fig. 4C to E; Fig. S7A). Using this workflow, we detected 36 out of 48 total clinical samples: 18/48 resulted as E484 (WT) and were subsequently tested with 452 and 501 gRNAs (3/18 called WT, 6/18 called Alpha, and 9/18 called Delta), 4/48 resulted as K484 (called Beta/Eta/Gamma/Iota/Mu/Zeta), 2/48 resulted as Q484 (called Kappa), and 12/48 resulted as A484 (called Omicron) (Fig. 4E; Fig. S7B to C). The remaining 12/48 clinical samples neither amplified nor showed any DETECTR signal and were thus called “not detected” (Data set S4).

Unblinding of samples COVID-92 through COVID-127 revealed five discordant samples: COVID-103, COVID-108, COVID-109, COVID-112, and COVID-122 (Fig. S7D). All five discordant samples were re-extracted from the original patient sample and reprocessed with WGS and COVID Variant DETECTR. After repeat testing, three samples (COVID-103, COVID-108, COVID-109) showed 100% concordance between WGS and DETECTR, with both methods resulting in “no call” at position 452. Notably, these samples were also part of the original set of 91 samples (COVID-20, COVID-63, COVID-73) that were previously concordant at position 452, suggesting a decrease in sample integrity likely resulting from multiple freeze/thaw cycles incurred during several re-extractions. Sample COVID-112 was called an Omicron by DETECTR based on its A484 SNP call, which was confirmed by WGS. Finally, sample COVID-122 could not be amplified by RT-LAMP, also suggesting a loss in sample integrity. Following this discrepancy analysis, we demonstrated an overall SNP concordance of 94.7%, and 100% NPA for this set of 48 samples (Fig. 4E).

The experimental design used for the first two sample sets focused on development and refinement of the data analysis pipeline, but incorporation of multiple biological and/or technical replicates per sample is not practical for most clinical laboratory workflows. Thus, we evaluated a third independent validation set of clinical samples ($n = 165$), processed as a single RT-LAMP reaction followed by a single DETECTR reaction for each SNP ($n = 8$ gRNAs) per clinical sample (Fig. 5A). Of the 165 clinical samples, 138 yielded DETECTR calls for all three SNPs and 27 showed incomplete or no SNP calls with DETECTR. After unblinding the viral WGS results, we found that 29 samples had produced insufficient coverage by viral WGS for lineage classification, which included eight samples that yielded incomplete SNP calls by DETECTR and two of the 138 samples that yielded DETECTR calls for all three SNPs. Therefore, these 29 samples were excluded from further analyses. Comparison of DETECTR SNP calls with viral WGS calls for the remaining 136 clinical samples showed 96.6% SNP agreement (394 of 408) with 13 discordant SNP calls among the nine discordant samples (Fig. S8A, S9). The sensitivities and specificities of the individual SNPs ranged from 95.7% to 100% and 96.3% to 100% (Fig. S8B). At the 484 position, A484, K484, and Q484 yielded 100% (35 of 35), 100% (2 of 2), and 66.7% (2 of 3) concordance, respectively, between the DETECTR assay and viral WGS (Fig. S8A).

Among the nine samples found to have SNP discordance, the lineage calls of only six of the patient samples were affected. To resolve these six lineage discrepancies, we analyzed the samples using a third comparator assay, a real-time RT-PCR run on a DiaSorin instrument. Two of the samples yielded an invalid result on the DiaSorin, likely secondary to low virus titers (cycle threshold, or Ct values ranging from 13 to 34) or sample integrity resulting from increased freeze/thaw cycles; these samples were excluded from the variant analyses. Of the remaining four samples with valid DiaSorin results, two were concordant with DETECTR only while two were concordant with viral WGS only (Fig. 5B; Fig. S8B to C), yielding 97% (132 of 134) agreement between

FIG 4 Legend (Continued)

specific detection of 484-specific mutations (E, K, Q, A) on PCR-amplified synthetic gene fragments ($n = 3$). (C) SARS-CoV-2 lineage classification table based on 484 mutations. (D) Alignment of final 484 mutation calls comparing the DETECTR and SARS-CoV-2 WGS assay results across 36 clinical samples. (E) Overall SNP concordance values for the 484 SNP from the evaluation of the DETECTR assay against the SARS-CoV-2 WGS comparator assay.

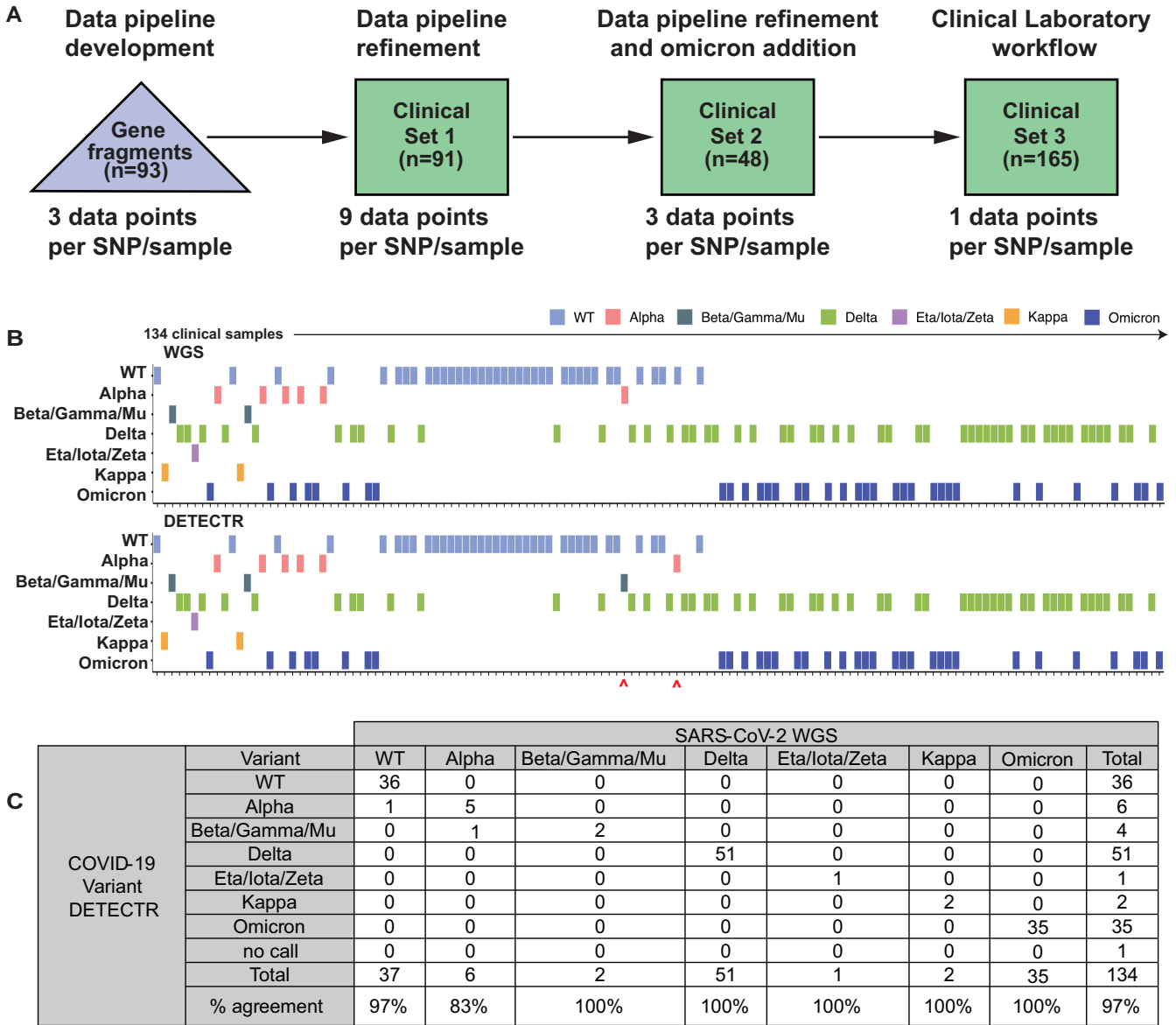


FIG 5 Testing of the COVID-19 variant DETECTR assay on a validation set of 165 clinical samples. Samples are processed according to a standard clinical laboratory workflow with no biological or technical replicates. (A) Schematic showing development of DETECTR workflow. (B) Final lineage classification by the DETECTR assay, after using viral WGS and DETECTR as assay comparators. Discordant calls are denoted with arrows. (C) Table showing the number of concordant samples (major diagonal from the upper left to lower right) and discordant samples (off the major diagonal) and overall agreement for each lineage classification.

DETECTR and two separate comparator assays overall (Fig. 5C). Based on available FDA guidance (54), we also analyzed a subset of 14 concordant samples between DETECTR and viral WGS using the DiaSorin assay. Results confirmed the lineage classification for all 14 samples (100% concordance among all three assays).

DISCUSSION

In this study, we developed a CRISPR-based DETECTR assay for the detection of SARS-CoV-2 variants. We evaluated three CRISPR-Cas12 enzymes, two commercially available (LbCas12a from NEB and AsCas12a from IDT) and one proprietary (CasDx1 from Mammoth Biosciences). Based on a head-to-head comparison of these enzymes, we observed clear differences in performance, with CasDx1 demonstrating the highest fidelity as the only enzyme able to reliably detect all targeted SNPs. A data analysis pipeline, developed to differentiate between WT and MUT signals with the DETECTR

assay, yielded an overall 97.3% SNP concordance (1,326 of 1,335 total SNP calls) and 98.9% agreement for lineage classification (258 of 261 samples) compared with viral WGS, with a third comparator DiaSorin variant assay used for discrepancy testing. These findings show robust agreement between DETECTR assay and viral WGS for identification of SNP mutations and variant categorization. Thus, the DETECTR assay provides a faster and simpler alternative to sequencing-based methods for COVID-19 variant diagnostics and surveillance.

Our results show that the choice of Cas enzyme is important to maximize the accuracy of CRISPR-based diagnostic assays and may need to be tailored to the site that is being targeted. As currently configured with the L452R, E484K/Q/A, and N501Y SNP targets, the COVID-19 variant DETECTR assay is currently capable of distinguishing the Alpha, Delta, Kappa, and Omicron variants, but cannot resolve the remaining VBMs or VOIs. However, given the rapid emergence and shifts in the distribution of variants over time (13) it is likely that tracking of key mutations, many of which are suspected to arise from convergent evolution (55), rather than tracking of variants, will be more important for surveillance as the pandemic continues. Here, we also developed a data analysis pipeline for CRISPR-based SNP calling that can readily incorporate additional targets and offers a blueprint for automated interpretation of fluorescent signal patterns.

Although CRISPR-based diagnostic assays have been previously demonstrated for the detection of SARS-CoV-2 variants, these studies have limitations regarding coverage of circulating lineages, the extent of clinical sample evaluation, and/or assay complexity. For example, the miSHERLOCK variant assay uses LbCas12a (NEB) with RPA pre-amplification to detect N501Y, E484K, and Y144Del covering eight lineages (WA-1, Alpha, Beta, Gamma, Eta, Iota, Mu, and Zeta) and was tested only on contrived samples (RNA spiked into human saliva) (21). The SHINEv2 assay uses LwaCas13a with RPA pre-amplification to detect 69/70Del, K417N/T, L452R, and 156/157Del + R158G covering eight lineages (WA-1, Alpha, Beta, Gamma, Delta, Epsilon, Kappa, and Mu) and was tested with only the 69/70Del gRNAs on 20 Alpha-positive NP clinical samples (56). Finally, the mCARMEN variant identification panel (VIP) uses 26 crRNA pairs with either the LwaCas13a or LbaCas13a and PCR pre-amplification to identify all current circulating lineages, including Omicron; however, the VIP requires the Fluidigm Biomark HD system or similar, more complex instrumentation for streamlined execution (57). In comparison, the DETECTR assay presented here uses CasDx1 with LAMP pre-amplification to detect N501Y, E484K/Q/A, and L452R covering all current circulating lineages, including Omicron, and was tested on 261 clinical samples representing eight lineages (WA-1, Alpha, Gamma, Delta, Epsilon, Iota, Mu, and Omicron). Furthermore, we demonstrate here that specific Omicron identification can be accomplished using only the E484 WT and A484 MUT guides.

Some limitations of our study are as follows. First, as previously mentioned, the DETECTR assay currently detects only the L452R, E484K/Q/A, and N501Y mutations, which may not provide enough resolution to identify future lineages. Second, we observed variable performance of the assay in SNP discrimination, with more potential overlap in the calls between WT and MUT for the 452 position than for the other two sites. These two limitations could potentially be addressed by the incorporation of additional gRNAs to the assay to provide specific and redundant coverage and to improve identification of specific lineages. Third, due to a multiplexed and degenerate S-gene LAMP primer design, the limit of detection of the DETECTR assay is higher than our previously published SARS-CoV-2 DETECTR assay (20), and thus only positive clinical samples with a Ct < 30 (near the limit of detection for viral whole-genome sequencing) were tested in our study. Incorporation of an additional N-gene target to the assay may be necessary if simultaneous detection and SNP/variant identification is desired. Finally, the current study focuses on the development and validation of a variant DETECTR assay using conventional laboratory equipment. Future work will involve implementation onto automated, portable systems for use in point of care settings.

In the near term, we suggest the use of the DETECTR assay as an initial screen for circulating variants and/or a distinct pattern from a rare or novel variant by interrogating the

key 452, 484, and 501 positions that could be reflexed to viral WGS. As the sequencing capacity for most clinical and public health laboratories is limited, the DETECTR assay would thus enable rapid identification of variants circulating in the community to support outbreak investigation and public health containment efforts. Identification of specific mutations associated with neutralizing antibody evasion (12, 58) could inform patient care with regard to the use of monoclonal antibodies that remain effective in treating the infection (15). As the virus continues to mutate and evolve, the DETECTR assay can be readily reconfigured by validating new gRNAs and pre-amplification LAMP primers and gRNAs that target emerging mutations with clinical and epidemiological significance. Thus, the assay would provide flexibility in testing for emerging variants amid a constantly changing pandemic landscape. Over the longer term, a validated CRISPR assay that combines SARS-CoV-2 detection with variant identification offers a faster and simpler alternative to sequencing and would be useful as a tool for simultaneous COVID-19 diagnosis in individual patients and surveillance for infection control and public health purposes.

SUPPLEMENTAL MATERIAL

Supplemental material is available online only.

SUPPLEMENTAL FILE 1, PDF file, 9 MB.

SUPPLEMENTAL FILE 2, XLSX file, 0.01 MB.

SUPPLEMENTAL FILE 3, XLSX file, 0.1 MB.

SUPPLEMENTAL FILE 4, XLSX file, 0.1 MB.

SUPPLEMENTAL FILE 5, XLSX file, 0.01 MB.

ACKNOWLEDGMENTS

We thank the UCSF Center for Advanced Technology core facility (Delsy Martinez and Tyler Miyasaki) for their efforts in high-throughput sequencing of viral cDNA libraries using the Illumina NovaSeq 6000 instrument, and Mary Kate Morris from the California Department of Public Health for providing the heat-inactivated viral cultures. We also thank Lucas Harrington and Teresa Peterson for their critical review of this manuscript.

This work has been funded by the Innovative Genomics Institute (IGI) at UC Berkeley and UC San Francisco (C.Y.C.), the Sandler Program for Breakthrough Biomedical Research (C.Y.C.), U.S. Centers for Disease Control and Prevention contract 75D30121C10991 (C.Y.C.), and Mammoth Biosciences.

C.L.F., J.S.C., and C.Y.C. conceived and designed the study; C.Y.C. and V.S. coordinated the SARS-CoV-2 whole-genome sequencing efforts and RT-LAMP primer design and testing; C.L.F., J.P.B., J.C., and J.S.C. designed guide RNAs for CRISPR-Cas12 testing; B.M., J.P.B., R.N.D., E.S., and C.G.H. tested guide RNAs and ran DETECTR experiments; V.S., N.B., B.W., A.S.-G., K.R., J.S., S.M., and C.Y.C. collected samples; C.L.F., V.S., B.M., V.N., J.P.B., J.C., J.S.C., and C.Y.C. analyzed data; C.L.F., V.S., V.N., B.M., J.P.B., J.C., J.S.C., and C.Y.C. wrote the manuscript. All authors read the manuscript and agree to its contents.

C.Y.C. is the director of the UCSF-Abbott Viral Diagnostics and Discovery Center and receives research support from Abbott Laboratories, Inc. C.L.F., B.M., V.N., J.P.B., R.N.D., E.S., C.G.H., J.C., and J.S.C. are employees of Mammoth Biosciences. C.Y.C. is a member of the scientific advisory board for Mammoth Biosciences. The other authors declare no competing interests.

REFERENCES

- Otto SP, Day T, Arino J, Colijn C, Dushoff J, Li M, Mechai S, Domselaar GV, Wu J, Earn DJD, Ogden NH. 2021. The origins and potential future of SARS-CoV-2 variants of concern in the evolving COVID-19 pandemic. *Curr Biol* 31:R918–R929. <https://doi.org/10.1016/j.cub.2021.06.049>.
- Walensky RP, Walke HT, Fauci AS. 2021. SARS-CoV-2 variants of concern in the United States—challenges and opportunities. *JAMA* 325:1037–1038. <https://doi.org/10.1001/jama.2021.2294>.
- Deng X, Gu W, Federman S, Du Plessis L, Pybus OG, Faria NR, Wang C, Yu G, Bushnell B, Pan C-Y, Guevara H, Sotomayor-Gonzalez A, Zorn K, Gopez A, Servellita V, Hsu E, Miller S, Bedford T, Greninger AL, Roychoudhury P, Starita LM, Famulare M, Chu HY, Shendure J, Jerome KR, Anderson C, Gangavarapu K, Zeller M, Spencer E, Andersen KG, MacCannell D, Paden CR, Li Y, Zhang J, Tong S, Armstrong G, Morrow S, Willis M, Matyas BT, Mase S, Kasirye O, Park M, Masinde G, Chan C, Yu AT, Chai SJ, Villarino E, Bonin B, Wadford DA, Chiu CY. 2020. Genomic surveillance reveals multiple introductions of SARS-CoV-2 into Northern California. *Science* 369:582–587. <https://doi.org/10.1126/science.abb9263>.
- Truelove S, Smith CP, Qin M, Mullany LC, Borchering RK, Lessler J, Shea K, Howerton E, Contamin L, Levander J, Salerno J, Hochheiser H, Kinsey M, Tallaksen K, Wilson S, Shin L, Rainwater-Lovett K, Lemaitre JC, Dent J, Kaminsky

- J, Lee EC, Perez-Saez J, Hill A, Karlen D, Chinazzi M, Davis JT, Mu K, Xiong X, Piontti AP, Vespignani A, Srivastava A, Porebski P, Venkatramanan S, Adiga A, Lewis B, Klahn B, Outten J, Schlitt J, Corbett P, Telionis PA, Wang L, Peddireddy AS, Hurt B, Chen J, Vullikanti A, Marathe M, Hoops S, Bhattacharya P, Machi D, Chen S, Paul R, Janies D, Thill J-C, et al. 2021. Projected resurgence of COVID-19 in the United States in July–December 2021 resulting from the increased transmissibility of the Delta variant and faltering vaccination. *Medrxiv*.
5. Washington NL, Gangavarapu K, Zeller M, Bolze A, Cirulli ET, Barrett KMS, Larsen BB, Anderson C, White S, Cassens T, Jacobs S, Levan G, Nguyen J, Ramirez JM, Rivera-Garcia C, Sandoval E, Wang X, Wong D, Spencer E, Robles-Sikisaka R, Kurzban E, Hughes LD, Deng X, Wang C, Servellita V, Valentine H, Hoff PD, Seaver P, Sathe S, Gietzen K, Sickler B, Antico J, Hoon K, Liu J, Harding A, Bakhtar O, Basler T, Austin B, MacCannell D, Isaksson M, Febbo PG, Becker D, Laurent M, McDonald E, Yeo GW, Knight R, Laurent LC, de Feo E, Worobey M, Chiu CY, et al. 2021. Emergence and rapid transmission of SARS-CoV-2 B.1.1.7 in the United States. *Cell* 184: 2587–2594.e7. <https://doi.org/10.1016/j.cell.2021.03.052>.
 6. Okereke M. 2021. Spread of the Delta Coronavirus variant: Africa must be on watch. *Public Health Pract (Oxf)* 2:100209. <https://doi.org/10.1016/j.puhip.2021.100209>.
 7. Sabino EC, Buss LF, Carvalho MPS, Prete CA, Crispim MAE, Fraiji NA, Pereira RHM, Parag KV, da Silva Peixoto P, Kraemer MUG, Oikawa MK, Salomon T, Cucunuba ZM, Castro MC, de Souza Santos AA, Nascimento VH, Pereira HS, Ferguson NM, Pybus OG, Kucharski A, Busch MP, Dye C, Faria NR. 2021. Resurgence of COVID-19 in Manaus, Brazil, despite high seroprevalence. *Lancet Lond Engl* 397:452–455. [https://doi.org/10.1016/S0140-6736\(21\)00183-5](https://doi.org/10.1016/S0140-6736(21)00183-5).
 8. Servellita V, Morris MK, Sotomayor-Gonzalez A, Gliwa AS, Torres E, Brazer N, Zhou A, Hernandez KT, Sankaran M, Wang B, Wong D, Wang C, Zhang Y, Reyes KR, Glasner D, Deng X, Streithorst J, Miller S, Frias E, Rodgers M, Cloherty G, Hackett J, Hanson C, Wadford D, Philip S, Topper S, Sachdev D, Chiu CY. 2022. Predominance of antibody-resistant SARS-CoV-2 variants in vaccine breakthrough cases from the San Francisco Bay Area, California. *Nat Microbiol* 7:277–212. <https://doi.org/10.1038/s41564-021-01041-4>.
 9. Kustin T, Harel N, Finkel U, Perchik S, Harari S, Tahor M, Caspi I, Levy R, Leshchinsky M, Dror SK, Bergerzon G, Gadban H, Gadban F, Eliassian E, Shimron O, Saleh L, Ben-Zvi H, Taraday EK, Amichay D, Ben-Dor A, Sagas D, Strauss M, Avni YS, Huppert A, Kepten E, Balicer RD, Netzer D, Ben-Shachar S, Stern A. 2021. Evidence for increased breakthrough rates of SARS-CoV-2 variants of concern in BNT162b2-mRNA-vaccinated individuals. *Nat Med* 27:1379–1384. <https://doi.org/10.1038/s41591-021-01413-7>.
 10. Jung J, Sung H, Kim S-H. 2021. Covid-19 breakthrough infections in vaccinated health care workers. *N Engl J Med* 385:1629–1631. <https://doi.org/10.1056/NEJMc2113497>.
 11. Brown CM, Vostok J, Johnson H, Burns M, Gharpure R, Sami S, Sabo RT, Hall N, Foreman A, Schubert PL, Gallagher GR, Fink T, Madoff LC, Gabriel SB, MacInnis B, Park DJ, Siddle KJ, Harik V, Arvidson D, Brock-Fisher T, Dunn M, Kearns A, Laney AS. 2021. Outbreak of SARS-CoV-2 infections, including COVID-19 vaccine breakthrough infections, associated with large public gatherings—Barnstable County, Massachusetts, July 2021. *MMWR Morb Mortal Wkly Rep* 70:1059–1062. <https://doi.org/10.15585/mmwr.mm7031e2>.
 12. Campbell F, Archer B, Laurenson-Schafer H, Jinnai Y, Konings F, Batra N, Pavlin B, Vandemaeele K, Kerkhove MDV, Jombart T, Morgan O, Le P de Waroux O. 2021. Increased transmissibility and global spread of SARS-CoV-2 variants of concern as at June 2021. *Eurosurveillance* 26:2100509. <https://doi.org/10.2807/1560-7917.ES.2021.26.24.2100509>.
 13. Harvey WT, Carabelli AM, Jackson B, Gupta RK, Thomson EC, Harrison EM, Ludden C, Reeve R, Rambaut A, Peacock SJ, Robertson DL, Consortium C-19 GU (COG-U). 2021. SARS-CoV-2 variants, spike mutations and immune escape. *Nat Rev Microbiol* 19:409–416. <https://doi.org/10.1038/s41579-021-00573-0>.
 14. Garcia-Beltran WF, Lam EC, Denis KSt, Nitido AD, Garcia ZH, Hauser BM, Feldman J, Pavlovic MN, Gregory DJ, Poznansky MC, Sigal A, Schmidt AG, lafrate AJ, Naranbhai V, Balazs AB. 2021. Multiple SARS-CoV-2 variants escape neutralization by vaccine-induced humoral immunity. *Cell* 184: 2523–2523. <https://doi.org/10.1016/j.cell.2021.04.006>.
 15. Focosi D, Tuccori M, Baj A, Maggi F. 2021. SARS-CoV-2 variants: a synopsis of in vitro efficacy data of convalescent plasma, currently marketed vaccines, and monoclonal antibodies. *Viruses* 13:1211. <https://doi.org/10.3390/v13071211>.
 16. Munnink BBO, Worp N, Nieuwenhuijse DF, Sikkema RS, Haagmans B, Fouchier RAM, Koopmans M. 2021. The next phase of SARS-CoV-2 surveillance: real-time molecular epidemiology. *Nat Med* 27:1518–1524. <https://doi.org/10.1038/s41591-021-01472-w>.
 17. Rockefeller Foundation. 2021. Toward a national genomic surveillance network. Rockefeller Foundation. <https://www.rockefellerfoundation.org/wp-content/uploads/2021/03/Toward-a-National-Genomic-Surveillance-Network-1.pdf>. Retrieved 28 January 2022.
 18. Harper H, Burridge A, Winfield M, Finn A, Davidson A, Matthews D, Hutchings S, Vipond B, Jain N, Edwards K, Barker G, Consortium TC-19 GU (COG-U). 2021. Detecting SARS-CoV-2 variants with SNP genotyping. *PLoS One* 16:e0243185. <https://doi.org/10.1371/journal.pone.0243185>.
 19. Verosloff MS, Shapiro SJ, Hawkins EM, Alpay E, Verma D, Stanfield EG, Kreindler L, Jain S, McKay B, Hubbell SA, Hendriks CG, Blizard BA, Broughton JP, Chen JS. 2021. CRISPR-Cas enzymes: the toolkit revolutionizing diagnostics. *Biotechnol J* 2100304. <https://doi.org/10.1002/biot.202100304>.
 20. Broughton JP, Deng X, Yu G, Fasching CL, Servellita V, Singh J, Miao X, Streithorst JA, Granados A, Sotomayor-Gonzalez A, Zorn K, Gopez A, Hsu E, Gu W, Miller S, Pan C-Y, Guevara H, Wadford DA, Chen JS, Chiu CY. 2020. CRISPR–Cas12-based detection of SARS-CoV-2. *Nat Biotechnol* 38: 870–874. <https://doi.org/10.1038/s41587-020-0513-4>.
 21. de Puig H, Lee RA, Najjar D, Tan X, Soekensen LR, Angenent-Mari NM, Donghia NM, Weckman NE, Ory A, Ng CF, Nguyen PQ, Mao AS, Ferrante TC, Lansberry G, Sallum H, Niemi J, Collins JJ. 2021. Minimally instrumented SHERLOCK (miSHERLOCK) for CRISPR-based point-of-care diagnosis of SARS-CoV-2 and emerging variants. *Sci Adv* 7:eabh2944. <https://doi.org/10.1126/sciadv.abh2944>.
 22. Patchsung M, Jantarug K, Pattama A, Aphicho K, Suraritdechachai S, Meesawat P, Sappakhaw K, Leelahakorn N, Ruenkam T, Wongsatit T, Athipanyasilp N, Eiamthong B, Lakkansirorat B, Phoodokmai T, Niljianskul N, Pakotiprapha D, Chanarat S, Homchan A, Tinikul R, Kamutira P, Phiwkao W, Soithongcharoen S, Kantiwiriyanitch C, Pongsupasa V, Trisrivirat D, Jaroensuk J, Wongnate T, Maenpuen S, Chaiyen P, Kamnerdnakta S, Swangsril J, Chuthapaisith S, Sirivatanauskorn Y, Chaimayo C, Sutthert R, Kantakamalakul W, Joung J, Ladha A, Jin X, Gootenberg JS, Abudayyeh OO, Zhang F, Horthongkham N, Uttamapinant C. 2020. Clinical validation of a Cas13-based assay for the detection of SARS-CoV-2 RNA. *Nat Biomed Eng* 4:1140–1149. <https://doi.org/10.1038/s41551-020-00603-x>.
 23. Fozouni P, Son S, Derby MD, de L, Knott GJ, Gray CN, D'Ambrosio MV, Zhao C, Switz NA, Kumar GR, Stephens SI, Boehm D, Tsou C-L, Shu J, Bhuiya A, Armstrong M, Harris AR, Chen P-Y, Osterloh JM, Meyer-Franke A, Joehnk B, Walcott K, Sil A, Langelier C, Pollard KS, Crawford ED, Puschnik AS, Phelps M, Kistler A, DeRisi JL, Doudna JA, Fletcher DA, Ott M. 2021. Amplification-free detection of SARS-CoV-2 with CRISPR-Cas13a and mobile phone microscopy. *Cell* 184:323–333.e9. <https://doi.org/10.1016/j.cell.2020.12.001>.
 24. FDA. 2020. SARS-CoV-2 RNA DETECTR assay. <https://www.fda.gov/media/139937/download>.
 25. FDA. 2020. Sherlock™ CRISPR SARS-CoV-2 kit. <https://www.fda.gov/media/137748/download>.
 26. FDA. DETECTR BOOST SARS-CoV-2 reagent kit. <https://www.fda.gov/media/155640/download>. Retrieved 28 January 2022.
 27. Gootenberg JS, Abudayyeh OO, Kellner MJ, Joung J, Collins JJ, Zhang F. 2018. Multiplexed and portable nucleic acid detection platform with Cas13, Cas12a, and Csm6. *Science* 360:439–444. <https://doi.org/10.1126/science.aag0179>.
 28. Chiu C. 2018. Cutting-edge infectious disease diagnostics with CRISPR. *Cell Host Microbe* 23:702–704. <https://doi.org/10.1016/j.chom.2018.05.016>.
 29. Chen JS, Ma E, Harrington LB, Costa MD, Tian X, Palefsky JM, Doudna JA. 2018. CRISPR-Cas12a target binding unleashes indiscriminate single-stranded DNase activity. *Science* 360:436–439. <https://doi.org/10.1126/science.aar6245>.
 30. Zhang L, Cui Z, Li Q, Wang B, Yu Y, Wu J, Nie J, Ding R, Wang H, Zhang Y, Liu S, Chen Z, He Y, Su X, Xu W, Huang W, Wang Y. 2021. Ten emerging SARS-CoV-2 spike variants exhibit variable infectivity, animal tropism, and antibody neutralization. *Commun Biol* 4:1196. <https://doi.org/10.1038/s42003-021-02728-4>.
 31. Kibbe WA. 2007. OligoCalc: an online oligonucleotide properties calculator. *Nucleic Acids Res* 35:W43–W46. <https://doi.org/10.1093/nar/gkm234>.
 32. Plitnick J, Griesemer S, Lasek-Nesselquist E, Singh N, Lamson DM, George KSt. 2021. Whole-genome sequencing of SARS-CoV-2: assessment of the ion torrent AmpliSeq panel and comparison with the Illumina MiSeq ARTIC protocol. *J Clin Microbiol* 59:e00649-21. <https://doi.org/10.1128/JCM.00649-21>.
 33. Quick J, Grubaugh ND, Pullan ST, Claro IM, Smith AD, Gangavarapu K, Oliveira G, Robles-Sikisaka R, Rogers TF, Beutler NA, Burton DR, Lewis-

- Ximenez LL, de Jesus JG, Giovanetti M, Hill SC, Black A, Bedford T, Carroll MW, Nunes M, Alcantara LC, Sabino EC, Baylis SA, Faria NR, Loose M, Simpson JT, Pybus OG, Andersen KG, Loman NJ. 2017. Multiplex PCR method for MinION and Illumina sequencing of Zika and other virus genomes directly from clinical samples. *Nat Protoc* 12:1261–1276. <https://doi.org/10.1038/nprot.2017.066>.
34. O'Toole Á, Scher E, Underwood A, Jackson B, Hill V, McCrone JT, Colquhoun R, Ruis C, Abu-Dahab K, Taylor B, Yeats C, Plessis LD, Maloney D, Medd N, Attwood SW, Aanensen DM, Holmes EC, Pybus OG, Rambaut A. 2021. Assignment of epidemiological lineages in an emerging pandemic using the pangolin tool. *Virus Evol* 7:veab064.
 35. Rambaut A, Holmes EC, O'Toole Á, Hill V, McCrone JT, Ruis C, Du Plessis L, Pybus OG. 2020. A dynamic nomenclature proposal for SARS-CoV-2 lineages to assist genomic epidemiology. *Nat Microbiol* 5:1403–1407. <https://doi.org/10.1038/s41564-020-0770-5>.
 36. R Core Team. 2018. R: A language and environment for statistical computing. R Core Team, Vienna, Austria. <https://www.r-project.org>.
 37. Corbett KS, Edwards DK, Leist SR, Abiona OM, Boyoglu-Barnum S, Gillespie RA, Himansu S, Schäfer A, Ziwawo CT, DiPiazza AT, Dinnon KH, Elbashir SM, Shaw CA, Woods A, Fritch EJ, Martinez DR, Bock KW, Minai M, Nagata BM, Hutchinson GB, Wu K, Henry C, Bahl K, Garcia-Dominguez D, Ma LZhi, Renzi I, Kong W-P, Schmidt SD, Wang L, Zhang Y, Phung E, Chang LA, Loomis RJ, Altaras NE, Narayanan E, Metkar M, Presnyak V, Liu C, Louder MK, Shi W, Leung K, Yang ES, West A, Gully KL, Stevens LJ, Wang N, Wrapp D, Doria-Rose NA, Stewart-Jones G, Bennett H, et al. 2020. SARS-CoV-2 mRNA vaccine design enabled by prototype pathogen preparedness. *Nature* 586: 567–571. <https://doi.org/10.1038/s41586-020-2622-0>.
 38. Polack FP, Thomas SJ, Kitchin N, Absalon J, Gurtman A, Lockhart S, Perez JL, Marc GP, Moreira ED, Zerbini C, Bailey R, Swanson KA, Roychoudhury S, Koury K, Li P, Kalina WV, Cooper D, Frenck RW, Hammitt LL, Türeci Ö, Nell H, Schaefer A, Ünal S, Tresnan DB, Mather S, Dormitzer PR, Şahin U, Jansen KU, Gruber WC, Group CCT. 2020. Safety and efficacy of the BNT162b2 mRNA COVID-19 vaccine. *New Engl J Medicine* 383:2603–2615. <https://doi.org/10.1056/NEJMoa2034577>.
 39. Bos R, Rutten L, van der Lubbe JEM, Bakkers MJG, Hardenberg G, Wegmann F, Zuidgeest D, de Wilde AH, Koornneef A, Verwilligen A, van Manen D, Kwaks T, Vogels R, Dalebout TJ, Myeni SK, Kikkert M, Snijder EJ, Li Z, Barouch DH, Vellinga J, Langedijk JPM, Zahn RC, Custers J, Schuitemaker H. 2020. Ad26 vector-based COVID-19 vaccine encoding a prefusion-stabilized SARS-CoV-2 Spike immunogen induces potent humoral and cellular immune responses. *NPJ Vaccines* 5:91. <https://doi.org/10.1038/s41541-020-00243-x>.
 40. Konings F, Perkins MD, Kuhn JH, Pallen MJ, Alm EJ, Archer BN, Barakat A, Bedford T, Bhiman JN, Caly L, Carter LL, Cullinane A, de Oliveira T, Druce J, Madry IE, Evans R, Gao GF, Gorbalenya AE, Hamblion E, Herring BL, Hodcroft E, Holmes EC, Kakkar M, Khare S, Koopmans MPG, Korber B, Leite J, MacCannell D, Marklewitz M, Maurer-Stroh S, Rico JAM, Munster VJ, Neher R, Munnink BO, Pavlin BI, Peiris M, Poon L, Pybus O, Rambaut A, Resende P, Subissi L, Thiel V, Tong S, van der Werf S, von Gottberg A, Ziebuhr J, Kerkhove MDV. 2021. SARS-CoV-2 variants of interest and concern naming scheme conducive for global discourse. *Nat Microbiol* 6: 821–823. <https://doi.org/10.1038/s41564-021-00932-w>.
 41. Malta F, de M, Amgarten D, Val FC, Cervato MC, Azevedo BMC, de Basqueira M, de S, Alves CO, dos S, Nobrega MS, de S Reis R, Sebe P, Gretsichschkin MC, Oliveira DDC, de Nakamura CNI, Chazanas PLN, Pinho JRR. 2021. Mass molecular testing for COVID19 using NGS-based technology and a highly scalable workflow. *Sci Rep* 11:7122. <https://doi.org/10.1038/s41598-021-86498-3>.
 42. Iglói Z, Velzing J, van Beek J, van de Vijver D, Aron G, Ensing R, Benschop K, Han W, Boelsums T, Koopmans M, Geurtsvankessel C, Molenkamp R. 2021. Clinical evaluation of Roche SD Biosensor Rapid Antigen Test for SARS-CoV-2 in municipal health service testing site, the Netherlands - Volume 27, Number 5—May 2021. *Emerg Infect Dis* 27:1323–1329. <https://doi.org/10.3201/eid2705.204688>.
 43. Broccanello C, Chiodi C, Funk A, McGrath JM, Panella L, Stevanato P. 2018. Comparison of three PCR-based assays for SNP genotyping in plants. *Plant Methods* 14:28. <https://doi.org/10.1186/s13007-018-0295-6>.
 44. McGuigan FEA, Ralston SH. 2002. Single nucleotide polymorphism detection: allelic discrimination using TaqMan. *Psychiatr Genet* 12:133–136. <https://doi.org/10.1097/00041444-200209000-00003>.
 45. Viana R, Moyo S, Amoako DG, Tegally H, Scheepers C, Althaus CL, Anyaneji UJ, Bester PA, Boni MF, Chand M, Choga WT, Colquhoun R, Davids M, Deforche K, Doolabh D, Du Plessis L, Engelbrecht S, Everatt J, Giandhari J, Giovanetti M, Hardie D, Hill V, Hsiao N-Y, Iranzadeh A, Ismail A, Joseph C, Joseph R, Koopile L, Pond SLK, Kraemer MUG, Kuate-Lere L, Laguda-Akingba O, Lesetedi-Mafoko O, Lessells RJ, Lockman S, Lucaci AG, Maharaj A, Mahlangu B, Maponga T, Mahlakwane K, Makatini Z, Marais G, Maruapala D, Masupu K, Matshaba M, Mayaphi S, Mbhele N, Mbulawa MB, Mendes A, Mlisana K, et al. 2022. Rapid epidemic expansion of the SARS-CoV-2 Omicron variant in southern Africa. *Nature* 1–10 603:679–686. <https://doi.org/10.1038/d41586-021-03832-5>.
 46. Flemming A. 2022. Omicron, the great escape artist. *Nat Rev Immunol* 22: 75–75. <https://doi.org/10.1038/s41577-022-00676-6>.
 47. VanBlargan LA, Errico JM, Halfmann PJ, Zost SJ, Crowe JE, Purcell LA, Kawaoka Y, Corti D, Fremont DH, Diamond MS. 2022. An infectious SARS-CoV-2 B.1.1.529 Omicron virus escapes neutralization by therapeutic monoclonal antibodies. *Nat Med* 28:490–495. <https://doi.org/10.1038/s41591-021-01678-y>.
 48. Hallett S. 2021. We need increased targeted measures now to slow the spread of omicron. *BMJ* 375:n3133. <https://doi.org/10.1136/bmj.n3133>.
 49. Majumdar S, Sarkar R. 2022. Mutational and phylogenetic analyses of the two lineages of the Omicron variant. *J Med Virol* 94:1777–1779. <https://doi.org/10.1002/jmv.27558>.
 50. Mertens J, Coppens J, Loens K, Mercier ML, Xavier BB, Lammens C, Vandamme S, Jansens H, Goossens H, Matheeußen V. 2022. Monitoring the SARS-CoV-2 pandemic: screening algorithm with single nucleotide polymorphism detection for the rapid identification of established and emerging variants. *Clin Microbiol Infect* 28:124–129. <https://doi.org/10.1016/j.cmi.2021.09.007>.
 51. Slenker A. 2022. Emerging variants of SARS-CoV-2 and novel therapeutics against coronavirus (COVID-19). StatPearls Publishing LLC.
 52. Feder KA, Patel A, Vepachedu VR, Dominguez C, Keller EN, Klein L, Kim C, Blood T, Hyun J, Williams TW, Feldman KA, Mostafa HH, Morris CP, Ravel J, Duwell M, Blythe D, Myers R. 2021. Association of E484K spike protein mutation with SARS-CoV-2 infection in vaccinated persons—Maryland, January – May 2021. *Clin Infect Dis* ciab762.
 53. Team CC-19 R. 2021. SARS-CoV-2 B.1.1.529 (Omicron) variant — United States, December 1–8, 2021. *Morbidity Mortal Wkly Rep* 70:1731–1734. <https://doi.org/10.15585/mmwr.mm7050e1>.
 54. FDA USD of Health and Human Services Food and Drug Administration, Center for Devices and Radiological Health. 2007. Statistical guidance on reporting results from studies evaluating diagnostic tests - guidance for industry and FDA staff.
 55. Singh J, Pandit P, McArthur AG, Banerjee A, Mossman K. 2021. Evolutionary trajectory of SARS-CoV-2 and emerging variants. *Virol J* 18:166. <https://doi.org/10.1186/s12985-021-01633-w>.
 56. Arizti-Sanz J, Bradley A, Zhang YB, Boehm CK, Freije CA, Grunberg ME, Kosoko-Thoroddsen T-SF, Welch NL, Pillai PP, Mantena S, Kim G, Uwanibe JN, John OG, Eromon PE, Kocher G, Gross R, Lee JS, Hensley LE, Happi CT, Johnson J, Sabeti PC, Myhrvold C. 2021. Equipment-free detection of SARS-CoV-2 and variants of concern using Cas13. *Medrxiv*.
 57. Welch NL, Zhu M, Hua C, Weller J, Mirhashemi ME, Mantena S, Nguyen TG, Shaw BM, Ackerman CM, Thakku SG, Tse MW, Kehe J, Bauer MR, Uwera M-M, Eversley JS, Bielwaski DA, McGrath G, Braidt J, Johnson J, Cerrato F, Petros BA, Gionet GL, Jalbert SK, Cleary ML, Siddle KJ, Happi CT, Hung DT, Springer M, MacInnis BL, Lemieux JE, Rosenberg E, Branda JA, Blainey PC, Sabeti PC, Myhrvold C. 2021. Multiplexed CRISPR-based microfluidic platform for clinical testing of respiratory viruses and SARS-CoV-2 variants. *Medrxiv*.
 58. Cao Y, Wang J, Jian F, Xiao T, Song W, Yisimayi A, Huang W, Li Q, Wang P, An R, Wang J, Wang Y, Niu X, Yang S, Liang H, Sun H, Li T, Yu Y, Cui Q, Liu X, Yang X, Du S, Zhang Z, Hao X, Shao F, Jin R, Wang X, Xiao J, Wang Y, Xie XS. 2022. Omicron escapes the majority of existing SARS-CoV-2 neutralizing antibodies. *Nature* 602:657–663. <https://doi.org/10.1038/s41586-021-04385-3>.